Article

TRANSPARENT PROCESS

EMBO reports

MicroRNA-independent functions of DGCR8 are essential for neocortical development and TBR1 expression

Federica Marinaro[1], Matteo J Marzi[2], Nadin Hoffmann[1], Hayder Amin[1], Roberta Pelizzoli[1], Francesco Niola[1], Francesco Nicassio[2] & Davide De Pietri Tonelli[1,*]

Abstract

Recent evidence indicates that the miRNA biogenesis factors DROSHA, DGCR8, and DICER exert non-overlapping functions, and have also roles in miRNA-independent regulatory mechanisms. However, it is currently unknown whether miRNA-independent functions of DGCR8 play any role in the maintenance of neuronal progenitors and during corticogenesis. Here, by phenotypic comparison of cortices from conditional *Dgcr8* and *Dicer* knockout mice, we show that *Dgcr8* deletion, in contrast to *Dicer* depletion, leads to premature differentiation of neural progenitor cells and overproduction of TBR1-positive neurons. Remarkably, depletion of miRNAs upon DCGR8 loss is reduced compared to DICER loss, indicating that these phenotypic differences are mediated by miRNA-independent functions of DGCR8. We show that *Dgcr8* mutations induce an earlier and stronger phenotype in the developing nervous system compared to *Dicer* mutants and that miRNA-independent functions of DGCR8 are critical for corticogenesis. Finally, our data also suggest that the Microprocessor complex, with DROSHA and DGCR8 as core components, directly regulates the *Tbr1* transcript, containing evolutionarily conserved hairpins that resemble miRNA precursors, independently of miRNAs.

Keywords Dgcr8; microRNAs; murine corticogenesis; neurogenesis; Tbr1
Subject Categories Neuroscience; RNA Biology
DOI 10.15252/embr.201642800 | Received 27 May 2016 | Revised 16 January 2017 | Accepted 19 January 2017 | Published online 23 February 2017
EMBO Reports (2017) 18: 603–618

Introduction

The mammalian neocortex is a complex laminar structure composed by multiple cell types that originates from the differentiation of neural progenitor cells (NPCs) in the telencephalon. Corticogenesis requires tight control of self-renewal, onset of cell fate commitment of NPCs, as well as differentiation, migration, maturation, and survival of their progeny. Understanding the precise regulation of intrinsic pathways and extrinsic factors that orchestrate these processes is crucial to achieve mechanistic insights of both cortical development and evolution [1,2].

MicroRNAs (miRNAs) are a class of ~22 nt in length, single-stranded non-coding RNAs that control the expression of the majority of protein coding genes (targets) [3–7] and are critical for corticogenesis and early postnatal development [8,9]. In mammals, canonical miRNAs are generally transcribed as immature (stem-loop containing) precursor RNAs that are cleaved by two RNAse-III proteins: DROSHA in the nucleus and DICER in the cytoplasm. Mature single-stranded miRNAs are then loaded onto the RNA-induced silencing complex (RISC) and bind to target mRNAs; by virtue of this interaction, miRNAs exert their post-transcriptional effect through repression of translation and/or stability of target mRNAs [10–12]. Conditional genetic knockouts of essential moieties for miRNA biogenesis, such as the "Microprocessor complex" (composed by the type III ribonuclease DROSHA and the RNA-binding protein DiGeorge syndrome critical region gene 8 (DGCR8), also known as PASHA), or the type III ribonuclease DICER [13–16] have been widely used to infer the global role of miRNAs in murine corticogenesis. Interestingly, global miRNA depletion by conditional ablation of *Dicer* leads to gross severe anatomical abnormalities in cortex as the result of impaired NPCs self-renewal, differentiation, and survival, depending from the developmental onset or cell type in which ablation occurs [9,17–20], indicating a crucial role of DICER for corticogenesis.

Although DROSHA, DGCR8, and DICER are essential for miRNA biogenesis, they also have non-overlapping functions [21–26]. These functions include, but are not limited to, non-canonical alternative miRNA biogenesis pathways that bypass the Microprocessor complex, but still depend on DICER [11] such as the direct modulation of RNA stability/transcription by the Microprocessor through miRNA-independent (and DICER-independent) mechanisms [27] or Microprocessor-dependent gene regulations that are independent of DROSHA RNA cleavage [28]. Some studies investigated the consequences of genetic ablation of *Dicer* versus *Dgcr8* for late-embryonic

1 Neuroscience and Brain Technologies Department, Istituto Italiano di Tecnologia, Genoa, Italy
2 Center for Genomic Science of IIT@SEMM, Istituto Italiano di Tecnologia, Milan, Italy
*Corresponding author. Tel: +39 010 71781 725; E-mail: davide.depietri@iit.it

and early postnatal mouse brain development [21,29] or upon knockdown of *Drosha* in embryonic mouse cortices [30], reporting that these non-overlapping functions impact on neuronal development. However, the specific contributions of these alternative pathways/functions to cortical neurogenesis still remain largely unknown. In particular, it is not known whether miRNA-independent functions of DGCR8 are involved in the maintenance of NPCs pools and their differentiation in corticogenesis. Thus, more comparative studies in which *Dgcr8*, *Drosha*, *Dicer,* or *Ago*(s) mutants are investigated in parallel are needed to understand the significance of these alternative functions *in vivo*.

Here, by conditional deletion of *Dgcr8* or *Dicer* genes in the mouse telencephalon, we study their specific and non-overlapping functions on corticogenesis, and in particular on proliferation/commitment of different NPCs subtypes and neurogenesis. Remarkably, conditional deletion of *Dgcr8* results in a more premature cortical impairment compared to *Dicer* ablation. Our results point out an essential miRNA-independent function of DGCR8 in corticogenesis that might be required for the regulation of target RNAs and suggest that *Tbr1* transcript might be one of such potential targets.

Results

Conditional ablation of *Dgcr8* in mouse cortical progenitors impairs corticogenesis

To study the role of DGCR8 in corticogenesis, we conditionally inactivated *Dgcr8* gene in apical progenitors cells (APs, a class of cortical NPCs that divide in the Ventricular Zone—VZ—in which we include neuroepithelial and radial glial cells) [1,31] before the onset of neurogenesis. To this aim, we crossed *Dgcr8*-flox mice [32] or *Dicer*-flox mice [33] with *Emx1*-Cre knock-in mice [34] and analyzed neocortical development in the resulting embryos (Fig 1A): wild type (WT), heterozygous for *Dgcr8*-flox allele (cHET), and conditional knockouts (cKO) for *Dicer*-flox (not shown) or *Dgcr8*-flox alleles. DGCR8 protein was completely depleted in E13.5 *Dgcr8* cKO cortices compared to control cortices (*Dgcr8* WT and cHET) of littermate embryos (Fig 1B and B'). Analysis of the gross morphology of postnatal brains of *Dgcr8* cKO mice revealed massive hypotrophy of the neocortex and olfactory bulbs, compared to both controls (Fig 1C), indicating a critical role of *Dgcr8* during corticogenesis.

The ablation of *Dicer* during corticogenesis was shown to induce massive apoptosis of NPCs and/or neurons [21,35–43]. Similarly, *Dgcr8* ablation in postmitotic neurons of the postnatal mouse neocortex was reported to induce cell death [21]. We therefore asked whether cell death occurs upon *Dgcr8* deletion in NPCs in our cKO mice. Analysis of cryosections through the dorsal telencephalon of E11.5 to E13.5 WT, *Dgcr8* cHET, and *Dgcr8* cKO mouse embryos revealed the presence of apoptotic cells from E12.5 in the *Dgcr8* cKO cortices, as revealed by pyknotic nuclei and immunoreactivity for activated caspase-3 [44] (Fig EV1A–C). Thus, consistently with our previous observations upon *Dicer* ablation [36], these results indicated that apoptosis is the main cause for the hypotrophy of the postnatal cortex in *Dgcr8* cKO mice.

We then investigated whether ablation of *Dgcr8* impaired NPCs expansion, taking into account only alive cells. Ventricular surface length is known to reflect the number of APs present in the VZ of the developing mouse neocortex [1,31]. We have previously shown that this parameter was not altered at E13.5 in *Emx1*-Cre *Dicer* cKO mice [36]. In order to ascertain whether this was also the case upon *Dgcr8* ablation, we measured ventricular surface length (Fig 1D and F), and cortical wall thickness (Fig 1E and G) in sections of WT, *Dgcr8* cHET, and *Dgcr8* cKO littermate embryos. The average ventricle length was significantly lower starting from E13.5 (Fig 1D and F), and the cortical wall thickness was significantly smaller at E12.5 (Fig 1E and G) in the telencephalon of *Dgcr8* cKO embryos compared to *Dgcr8* controls. Given that the ventricular surface length in *Dgcr8* cKO cortices was reduced at E13.5, while it was not altered in age-matched *Dicer* cKO embryos [36], this result opened the possibility of differential requirements for DGCR8 and DICER for corticogenesis.

Impairment of corticogenesis is more pronounced and premature upon deletion of *Dgcr8* than *Dicer*

Next, we investigated the architecture and relative proportions of the cortical plate (CP) and progenitors layers (i.e., VZ, and the subventricular zone, SVZ) in *Dgcr8*- versus *Dicer*-ablated cortices (Fig 2). Immunofluorescence staining for Tuj1 (pan-neuronal marker βIII-tubulin) [45] and Sox2 (stem and progenitor cells marker) [46] was used to identify CP neurons or VZ/SVZ progenitors, respectively. Consistently with previous data [36], a reduction in the neuronal layers thickness was among the earliest detectable phenotypes in the dorsal telencephalon of E13.5 *Dicer* cKO mouse embryos (Fig 2D–D''' and E) compared to WT (Fig 2A–A''' and E). In contrast, the structure of the telencephalon was dramatically disorganized in *Dgcr8* cKO embryos (Fig 2C–C''' and E) compared to both *Dicer* cKO (Fig 2D–D''' and E) and controls cortices (Fig 2A–B''' and E). Remarkably, thickness of *Dgcr8* cKO cortices (Fig 2C–C''' and E)

Figure 1. Conditional ablation of *Dgcr8* by *Emx1*-Cre impairs corticogenesis.

A Genotyping of the animals used in this study.

B, B' Western blot and quantification of DGCR8 and actin expression in E13.5 WT, *Dgcr8* cHET, and cKO cortices. Bars are mean ± SEM of three embryos per condition. One-way ANOVA, $*P < 0.05$; $**P < 0.01$.

C Brains from P7 WT, *Dgcr8* cHET, and cKO mice. Mb, midbrain: Cx, cortex (white dashed line); OB, olfactory bulb.

D, E WT, *Dgcr8* cHET, and cKO dorsal telencephalon sections stained with Hoechst. Asterisks indicate the ventricular lumen. Scale bars: 200 μm (D) and 50 μm (E).

F Quantification of the lateral ventricle surface length (i.e., indicated by the two arrowheads in D) from E11.5 to E13.5. Bars are mean ± SEM of three embryos per condition (18 counted fields per condition). Two-way ANOVA followed by Tukey's *post hoc* test, $*P < 0.05$; $**P < 0.01$; n.s., not significant.

G Quantification of the cortical thickness at embryonic days E11.5 and E12.5. Bars are mean ± SEM of three embryos per condition (18 counted fields per condition). Two-way ANOVA followed by Tukey's *post hoc* test, $*P < 0.05$; $**P < 0.01$; n.s., not significant.

was more reduced than *Dicer* cKO cortices (Fig 2D–D''' and E). Moreover, the onset of cortical disorganization was already detectable at E11.5 in *Dgcr8* cKO mice (Appendix Fig S1).

To ascertain whether these phenotypes might arise from different stability of *Dgcr8* versus *Dicer* transcripts upon genetic ablation, we quantified their levels in cortices of E13.5 cKO mice and respective

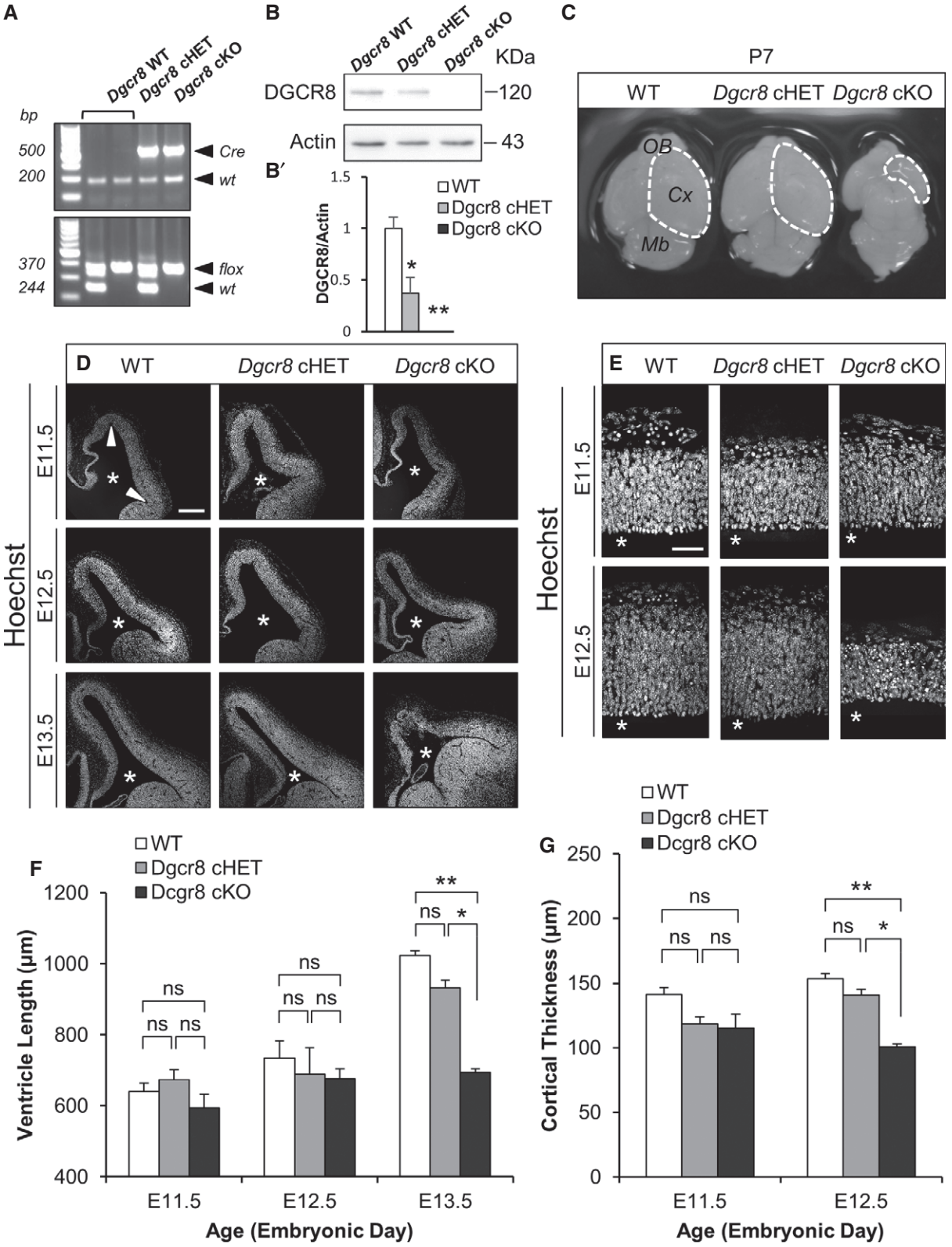

Figure 1.

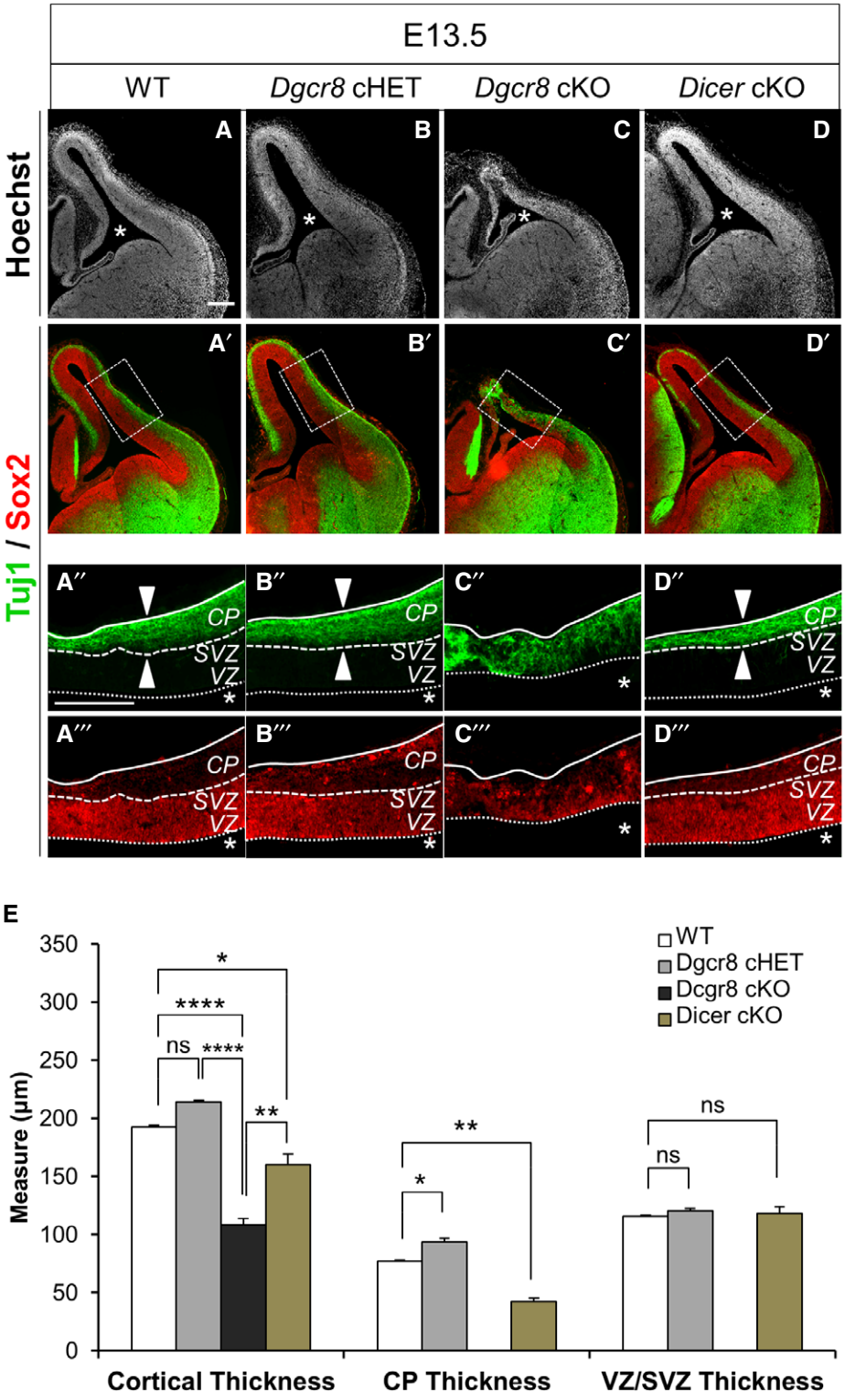

Figure 2. ***Dgcr8*** **ablation leads to loss of cortical architecture, while** ***Dicer*** **ablation leads to reduction in neuronal layers.**

A–D‴ Tuj1 and Sox2 immunofluorescence microscopy images of coronal cryosections through the dorsal telencephalon of E13.5 WT (A, A′), *Dgcr8* cHET (B, B′), *Dgcr8* cKO (C, C′), and *Dicer* cKO (D, D′) mouse embryos. (A″–D‴) Higher magnification of the brain regions indicated with the dashed boxes in (A′–D′). Scale bar: 200 µm. Asterisks indicate the ventricular lumen. Solid and dashed lines indicate cortex boundaries; white arrowheads indicate cortical plate thickness. Cortical plate (CP); subventricular zone (SVZ); ventricular zone (VZ).

E Quantification of the areas of the cortical thickness, the neuronal layer (CP, Tuj1$^+$), and of the germinative (progenitor) layers (VZ/SVZ, Sox2$^+$) from (A″–D‴). Bars are mean ± SEM of three embryos per condition (18 counted fields per condition). One-way ANOVA, *$P < 0.05$; **$P < 0.01$; ****$P < 0.0001$; n.s., not significant.

WT littermates by qRT–PCR. This quantification revealed a more dramatic reduction in *Dicer* transcript than *Dgcr8* (Fig EV2A and B). Interestingly, by *in situ* hybridization we found that *Dgcr8* mRNA expression was enriched in the VZ/SVZ (Fig EV2C), while *Dicer* was expressed throughout the cortical wall (Fig EV2D). Enrichment of *Dgcr8* mRNA expression in VZ/SVZ was already detectable at E11.5 and persisted throughout the analyzed stages (Fig EV2E), while its expression in the CP appeared only at E15.5, at lower levels compared to those of VZ/SVZ (Fig EV2E; VZ, CP). These results demonstrate, for the first time in the nervous system, a more premature and pronounced effect upon genetic ablation of *Dgcr8* than *Dicer* and suggest a role of *Dgcr8* for the maintenance of NPCs pools and/or differentiation during corticogenesis.

Dgcr8 deletion in developing cortex results in increased generation of Tbr1$^+$ neurons

In order to investigate the effect of *Dgcr8* deletion for the maintenance and/or differentiation of cortical progenitor pools, we quantified the proportions of apical (APs) and basal (intermediate) progenitors (BPs, progenitors that originate from APs, delaminate from the VZ and divide in the SVZ, in which we include basal progenitors, basal/outer radial glia, and subapical progenitors) [1,31] and differentiated neurons (Figs 3 and EV3). To this end, we performed immunostaining for the transcription factors Pax6, Tbr2 and Tbr1, markers of APs, BPs, and neurons, respectively [47–49], in sections of the dorsal telencephalon of E13.5 WT, *Dgcr8* cHET, and *Dgcr8* cKO mouse embryos (Fig EV3). Interestingly, though we did not find differences in the relative proportions of Pax6$^+$ or Tbr2$^+$ progenitors in cortices of the three *Dgcr8* genotypes (Fig EV3A–H), the proportion of Tbr1$^+$ cells was increased threefold in *Dgcr8* cKO cortices compared to control embryos (Fig EV3I–L). Moreover, Tbr1$^+$ cells were scattered through the cortical wall of *Dgcr8* cKO embryonic cortices (Fig EV3K), in parallel with short and disorganized APs as revealed by immunostaining for radial glial cell marker Nestin (Fig EV3M and N). This result suggests that VZ derangement is the main cause of Tbr1$^+$ cells misplacement upon depletion of DGCR8. The neuronal identity of Tbr1$^+$ cells in *Dgcr8* cKO embryos was confirmed by co-staining with Tuj1 and by lack of co-labeling with the proliferation marker Mcm2 [50] (Appendix Fig S2).

In order to ascertain whether the increased proportion of Tbr1$^+$ neurons upon *Dgcr8* ablation might have resulted from increased neurogenesis, we administered Bromodeoxyuridine (BrdU) in WT, *Dgcr8* cHET, and *Dgcr8* cKO embryos at E12.5 and quantified the proportion of Tbr1$^+$/BrdU$^+$ double-positive neurons in the dorsal telencephalon at E13.5 (Fig 3A–C' and G, and Appendix Fig S3A). This quantification revealed a fivefold increase in the proportion of Tbr1$^+$/BrdU$^+$ neurons over total BrdU$^+$ cells in *Dgcr8* cKO embryos (Fig 3C–C' and G, green bar), compared to *Dgcr8* controls (Fig 3A–B' and G, green bars). In the same embryos, we quantified proportion of Tbr2$^+$/BrdU$^+$ BPs over total BrdU$^+$ cells (Fig 3D–G and Appendix Fig S3B) and found that it was significantly higher in *Dgcr8* cKO cortices (Fig 3F–G, pink bars) compared to *Dgcr8* controls (Fig 3D–E' and G, pink bars). Finally, to extrapolate the proportion of APs generated during 24 h from BrdU administration,

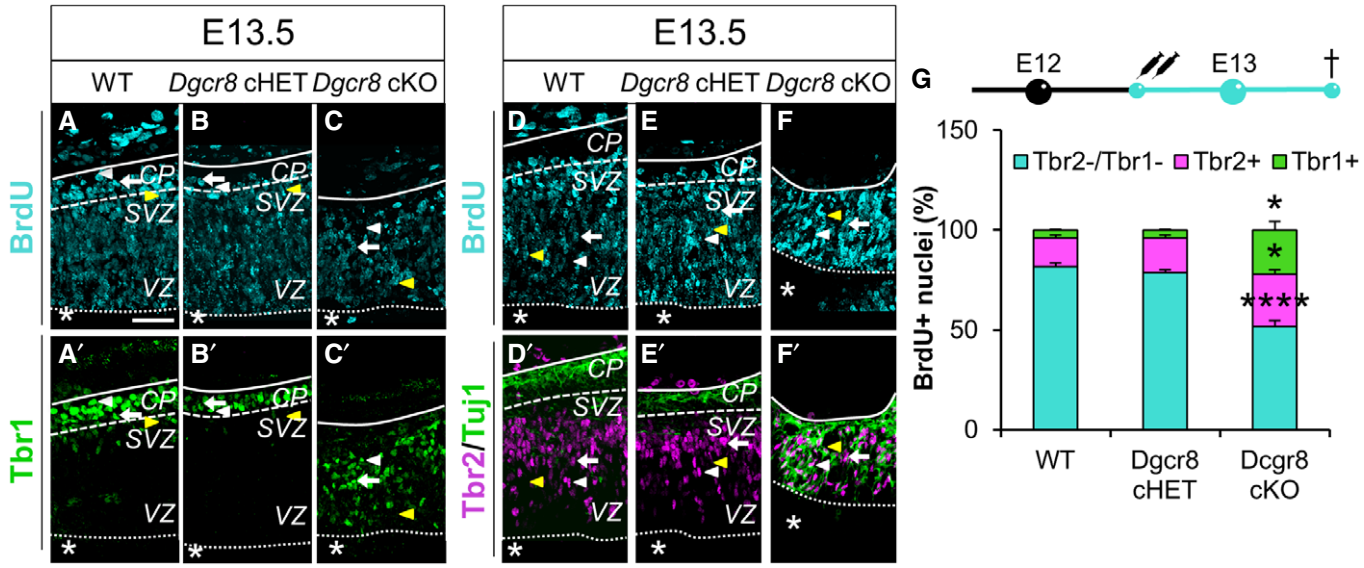

Figure 3. *Dgcr8* ablation leads to increased generation of Tbr1$^+$ neurons.

A–F' Immunofluorescence microscopy of coronal cryosections through the dorsal telencephalon of E13.5 WT (A, A', D, D'), *Dgcr8* cHET (B, B', E, E'), and *Dgcr8* cKO (C, C', F, F') littermate mouse embryos, subjected to two BrdU administrations from E12.5. Double immunostaining for BrdU (A–F, cyan) and Tbr1 (A'–C', green), or triple immunostaining for BrdU, Tbr2 (D'–F', magenta), and Tuj1 (D'–F', green). Arrowheads and arrows indicate categories of counted cells as shown in Appendix Fig S3. Asterisks indicate the ventricular lumen. Solid and dashed lines indicate cortex boundaries. Cortical plate (CP); subventricular zone (SVZ); ventricular zone (VZ). Scale bars: 50 μm.

G BrdU injection scheme (up) and quantification (down) of the proportions of Tbr1$^+$ neurons (BrdU$^+$/Tbr1$^+$, green bars), Tbr2$^+$ basal progenitors (BrdU$^+$/Tbr2$^+$, pink bars), and apical progenitors (BrdU$^+$/Tbr1$^-$/Tbr2$^-$, cyan bars) generated in 24 h in similar sections as shown in (A–F'). Apoptotic nuclei are excluded from all the quantifications. Bars are mean ± SEM of three embryos per condition (18 counted fields per condition). One-way ANOVA, *$P < 0.05$; ****$P < 0.0001$.

we quantified Tbr2$^-$/Tbr1$^-$/BrdU$^+$ cells over total BrdU$^+$ cells in the same sections and found that this proportion was significantly lower in *Dgcr8* cKO cortices compared to *Dgcr8* controls (Fig 3G, cyan bars). These data indicate that *Dgcr8* ablation increases the generation of Tbr1$^+$ neurons and unbalances maintenance of APs/BPs pools between E12.5 and E13.5.

Opposite effects of *Dgcr8* ablation on proliferation of Tbr2$^+$ BPs and Pax6$^+$ APs

To ascertain which subtype of NPCs was responsible for the overproduction of Tbr1$^+$ neurons in *Dgcr8* cKO cortices, we investigated the proliferation of APs and BPs in the dorsal telencephalon of E13.5 WT, *Dgcr8* cHET, and *Dgcr8* cKO embryos by short BrdU pulses (Fig 4A–G' and Appendix Fig S3C and D). This analysis revealed an increased proportion of Pax6$^+$/BrdU$^+$ double-positive cells over the total Pax6$^+$ APs in cortices from *Dgcr8* cHET (Fig 4B–B' and G, cyan bar) and *Dgcr8* cKO embryos (Fig 4C–C' and G, cyan bar), compared to WT littermates (Fig 4A–A' and G, cyan bar). In contrast, the proportion of Tbr2$^+$/BrdU$^+$ double-positive cells over the total Tbr2$^+$ BPs was decreased in cortices of *Dgcr8* cKO embryos (Fig 4F–G', cyan bar) compared to both *Dgcr8* controls (Fig 4D–E' and G', cyan bars). These results indicate that BPs decrease their proliferation while APs increase it upon *Dgcr8* ablation. Given that neurogenic NPCs have a longer cell cycle than proliferative ones [51,52], we concluded that premature differentiation of Tbr2$^+$ BPs cells was accounting for the overproduction of Tbr1$^+$ neurons in *Dgcr8*-ablated cortices. We postulate that the increased proliferation of APs (Fig 4G) might represent a compensatory feedback response to BPs drain, thus leading to APs premature consumption (Fig 3G).

Upregulation of Tbr1 in newborn cortical neurons is not preceded by changes in Ngn2 expression and is paralleled by defective laminar fate specification in *Dgcr8* depleted cortices

The sequential transcriptional cascade of Pax6, Tbr2, and Tbr1 characterizes cortical neurogenesis [48]. The transcription factor Ngn2 is one of the main regulators acting at the top of this cascade. Both Tbr2 and Tbr1 are under the control of Ngn2 [53,54]: in developing mice, overexpression of *Ngn2* was shown to induce the expression of Tbr1 [54] and *Ngn2*$^{-/-}$ mutants display reduced Tbr1 expression. In addition, *Ngn2* mRNA is destabilized by DROSHA during corticogenesis through a miRNA-independent post-transcriptional mechanism [30]. In order to investigate whether altered expression of

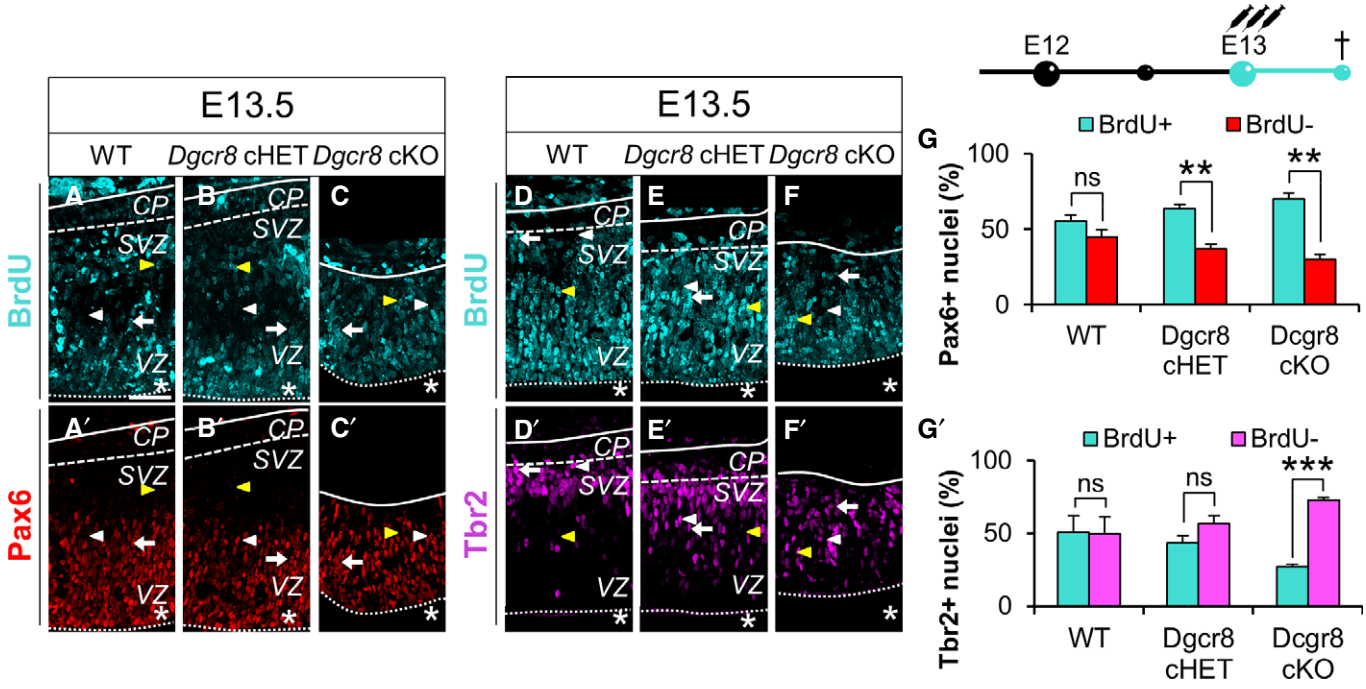

Figure 4. Decreased proliferation of Tbr2$^+$ BPs and increased proliferation of Pax6$^+$ APs in *Dgcr8* cKO cortices.

A–F' Immunofluorescence microscopy of coronal cryosections through the dorsal telencephalon of E13.5 WT (A, A', D, D'), *Dgcr8* cHET (B, B', E, E'), and *Dgcr8* cKO (C, C', F, F') littermate mouse embryos, subjected to three BrdU administrations from E13.0. Double immunostaining for BrdU (A–F, cyan) and Pax6 (A'–C', red) or Tbr2 (D'–F', magenta). Arrowheads and arrows indicate categories of counted cells as shown in Appendix Fig S3.

G BrdU injection scheme (up) and quantification (down) of the proportions of proliferating (BrdU$^+$/Pax6$^+$, cyan bars) and not proliferating apical progenitors (BrdU$^-$/Pax6$^+$, red bars) in similar sections as shown in (A–C'). Asterisks indicate the ventricular lumen. Solid and dashed lines indicate cortex boundaries. Cortical plate (CP); subventricular zone (SVZ); ventricular zone (VZ). Scale bars: 50 μm.

G' Quantification of the proportions of proliferating (BrdU$^+$/Tbr2$^+$, cyan bars) and not proliferating basal progenitors (BrdU$^-$/Tbr2$^+$, pink bars) in similar sections as shown in (D–F').

Data information: (G, G') Apoptotic nuclei are excluded from all the quantifications. Bars are mean ± SEM of three embryos per condition (18 counted fields per condition). One-way ANOVA, $^{**}P < 0.01$; $^{***}P < 0.001$; n.s., not significant.

Ngn2 in NPCs could account for the increased number of $Tbr1^+$ neurons and/or for the unbalance of APs/BPs pools observed upon *Dgcr8* ablation, we quantified the proportion of $Ngn2^+$ cells in cortices of E12.5 WT, *Dgcr8* cHET, and cKO embryos and found no difference (Fig 5A–D). This result indicates that altered Ngn2 expression does not account for the increased generation of $Tbr1^+$ neurons in *Dgcr8*-depleted cortices.

During corticogenesis, subsequent waves of cortical projection neurons are specified and born accumulating in an "inside-out" pattern in the growing cortical plate, thus giving rise to the six-layered structure of the mammalian neocortex [55]. Tbr1 is known to directly regulate the specification of the deep-layer six neurons and to orchestrate, together with Ctip2 and Sox5, the laminar fate choices of newly generated cortical neurons [49,56]. To investigate whether laminar fate specification of $Tbr1^+$ neurons was altered upon *Dgcr8* ablation, we examined the expression of the transcription factors Ctip2 and Sox5, markers of deep-layer neurons [57] in cortices of E13.5 WT, *Dgcr8* cHET, and *Dgcr8* cKO embryos (Fig 5E–L). This analysis revealed a strong decrease in the proportion of both $Ctip2^+$ (Fig 5G and H) and $Sox5^+$ (Fig 5K and L) neurons in *Dgcr8* cKO compared to *Dgcr8* control embryos (Fig 5E, F, H–J and L).

In sum, these results indicate that *Dgcr8* ablation increases generation of Tbr1 positive neurons without changes in Ngn2 expression and alters laminar fate specification of newborn cortical neurons.

miRNA-independent functions of DGCR8 are required for proper corticogenesis

To identify the molecular mechanisms underlying the phenotypes observed in *Dgcr8*-ablated cortices, we first asked whether miRNAs depletion in cortices of *Dgcr8* and *Dicer* cKOs embryos paralleled the severity of the respective phenotypes (Fig 2). To this aim, we isolated total RNA from E13.5 WT, *Dgcr8* cHET, *Dgcr8* cKO, and *Dicer* cKO cortices and analyzed libraries of the small RNAs fraction by deep sequencing. Remarkably, we found (out of the total genome-aligned small RNAs reads obtained in the different libraries; Fig 6A) a more severe depletion of total miRNA reads (i.e., ~75% decrease) in *Dicer* cKO, compared to *Dgcr8* cHET (i.e., ~15% decrease) and *Dgcr8* cKO (~35% decrease) (Fig 6B). These results were consistent with previous profiling of miRNAs from *Dicer*- and *Dgcr8*-ablated mouse embryonic stem (ES) cells and postnatal brains [21–23]. Remarkably, given that the severity of the phenotypes observed in *Dgcr8* and *Dicer* cKO cortices (Fig 2) was inversely proportional to the residual miRNAs upon *Dgcr8* and *Dicer* deletion (Fig 6B), we postulate that the molecular mechanisms underlying DGCR8 functions in corticogenesis are likely miRNA-independent.

Next, we also analyzed our libraries to determine DGCR8 vs. DICER responsiveness of the genome-aligned miRNA sequence reads. Reasoning that *Dicer* ablation inhibits the biogenesis of nearly all (canonical and non-canonical) miRNAs, while ablation of *Dgcr8* inhibits the biogenesis of canonical miRNAs only [11,58], we plotted the expression fold-change values (log_2) between each mutant versus WT, and classified miRNAs into four categories according to their responsiveness to DGCR8 and/or DICER (Fig 6C and D). This analysis revealed that the majority of miRNAs (i.e., 58% of reads) were responsive to both DICER and DGCR8, and thus, we classified this group as "canonical miRNAs". Another group of miRNAs was *Dgcr8* non-responsive and *Dicer*-responsive and thus defined as "non-canonical miRNAs". In total, we identified 39 *bona fide* non-canonical miRNAs (Table EV1). Consistently, eight of them (Fig EV4) were previously classified as non-canonical miRNAs also in ES cells or in postmitotic neurons [21–23,25,59].

DGCR8 regulates Tbr1 expression independent of miRNAs

Alternative miRNA-independent functions of the Microprocessor have been previously reported in other contexts [21,24,26,30,60–65]. In particular, it has been shown that the Microprocessor protein DROSHA, by cleaving hairpin structures resembling those of pri-miRNAs, can regulate RNA transcripts independently of miRNAs, eventually leading to RNA target destabilization [30,58,60,66–68].

Altered Ngn2 level could not account for the increased expression of Tbr1 observed in *Dgcr8* cKO cortices (Figs 3, 5, and EV3), suggesting that Tbr1 expression might be regulated at the post-transcriptional level. Thus, it is possible to hypothesize that DGCR8 loss might cause depletion of some critical miRNAs for Tbr1 expression that DICER loss does not, or in alternative that *Tbr1* mRNA could be a target of miRNA-independent DGCR8-dependent function.

We first analyzed the expression levels of the experimentally supported miRNAs known to target *Tbr1* mRNA (TarBase, Fig 7A) or predicted to target *Tbr1* (Targetscan, miRanda, Appendix Fig S4). We found that all these miRNAs were more downregulated in *Dicer* cKO compared to *Dgcr8* cKO cortices (Fig 7A and Appendix Fig S4), thus excluding loss of this subset of miRNAs as cause of increased Tbr1 expression. Next, in order to ascertain whether *Dgcr8* manipulation can modulate Tbr1 expression levels, we overexpressed *Dgcr8*

Figure 5. *Dgcr8* ablation does not alter Ngn2 levels, but downregulates Ctip2 and Sox5 expression in newborn neurons.

A–C Immunofluorescence microscopy of coronal cryosections through the dorsal telencephalon of E12.5 WT, *Dgcr8* cHET, and *Dgcr8* cKO littermate mouse embryos, showing Ngn2 (green) staining.

D Quantification of the proportion of $Ngn2^+$ cells, expressed as a percentage of the total Hoechst-stained nuclei (not shown).

E–G Immunofluorescence microscopy of coronal cryosections through the dorsal telencephalon of E13.5 WT, *Dgcr8* cHET, and *Dgcr8* cKO littermate mouse embryos, showing Ctip2 (yellow) staining.

H Quantification of the proportion of $Ctip2^+$ neurons, expressed as a percentage of the total Hoechst-stained nuclei (not shown).

I–K Immunofluorescence microscopy of coronal cryosections through the dorsal telencephalon of E13.5 WT, *Dgcr8* cHET, and *Dgcr8* cKO littermate mouse embryos, showing Sox5 (cyan) staining.

L Quantification of the proportion of $Sox5^+$ neurons, expressed as a percentage of the total Hoechst-stained nuclei (not shown).

Data information: Scale bars: 50 μm. Asterisks indicate the ventricular lumen. Solid and dashed lines indicate cortex boundaries. Cortical plate (CP); subventricular zone (SVZ); ventricular zone (VZ). Pyknotic apoptotic nuclei are excluded from all the quantifications. Bars are mean ± SEM of three embryos per condition (18 counted fields per condition). One-way ANOVA, $*P < 0.05$; $***P < 0.001$; n.s., not significant.

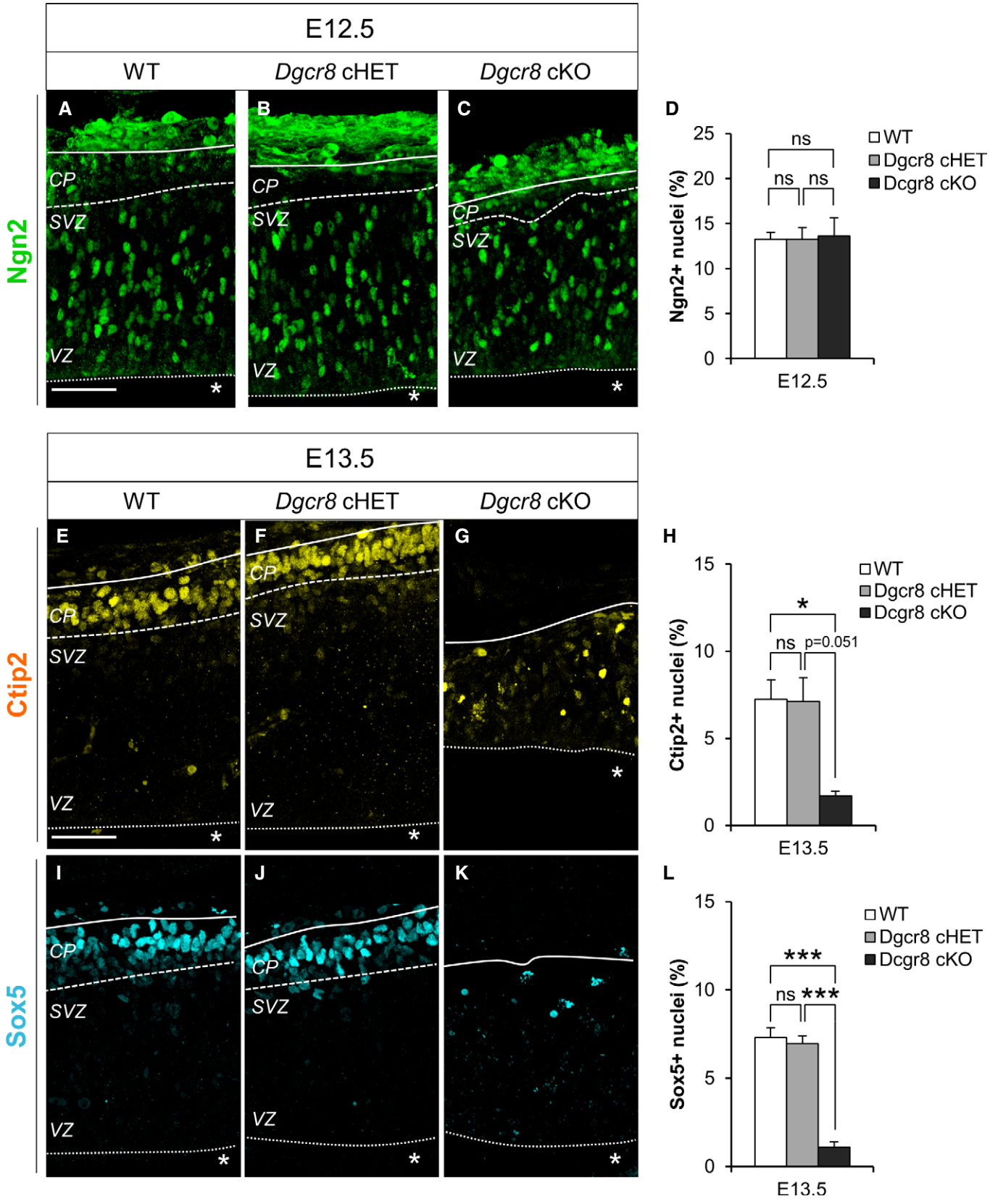

Figure 5.

A

	aligned reads	miR-reads
Dicer WT	4,974,224	2536724.5
Dicer cKO	1,087,377	490971.5
Dgcr8 WT	2,979,221	1,561,855
Dgcr8 cKO	2,149,924	1,122,529

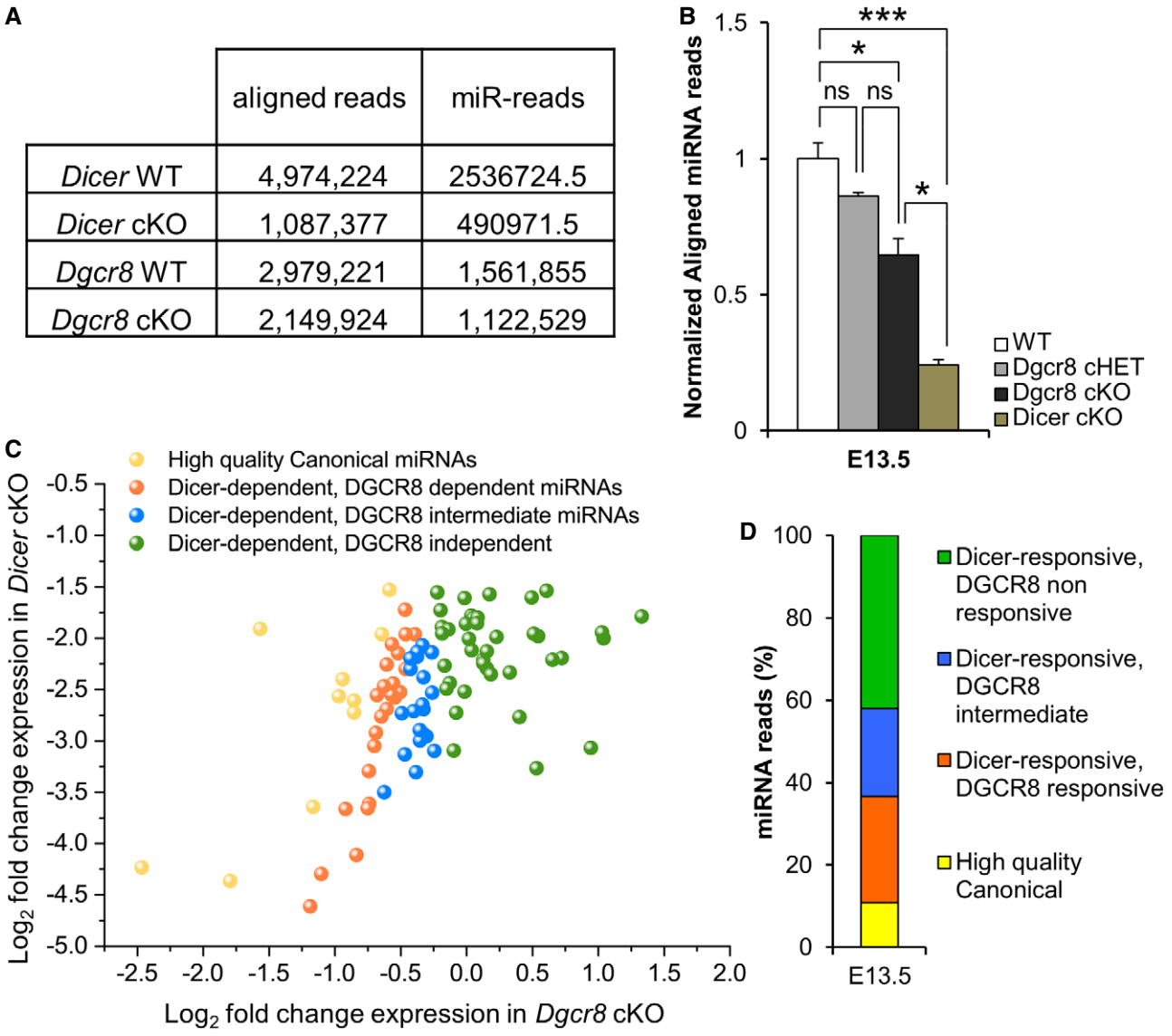

Figure 6. Aligned miRNA reads in normalized libraries from *Dicer* cKO and *Dgcr8* cKO E13.5 embryonic neocortex.

A Unique, genome-mapping reads from each library.

B Read counts for all genome-aligned miRNA sequences identified in WT, *Dgcr8* cHET, *Dgcr8* cKO, and *Dicer* cKO E13.5 cortices. Data are the mean of 2–4 libraries per condition; bars indicate the variation of the cortices from the mean (SEM). One-way ANOVA, $*P < 0.05$; $***P < 0.001$; n.s., not significant.

C Each axis indicates the following quotient: read counts from mutant library/read count from wild-type library, with read counts normalized to the number of snoRNA-derived reads from that library. Log_2 fold regulation decrease < 1.5 in *Dicer* cKO libraries and < 0.25 in *Dgcr8* cKO libraries defined enzyme dependence. miRNAs were categorized in consideration of their dependencies on both Dicer and DGCR8, and are color coded according to the key.

D Fraction (expressed as the % over the total number of miRNAs identified) of Dicer-responsive, differentially DGCR8-responsive miRNAs annotated from miRBase release 20.

in murine N2A cells. Two days post-transfection, we found that DGCR8 overexpression leads to decrease in TBR1 protein level (Fig 7B), indicating the DGCR8 can regulate Tbr1 expression in these cells.

We then searched for evolutionarily conserved secondary structures within *Tbr1* mRNA following a previously published approach [30] and found five predicted evolutionarily conserved stem-loop hairpin structures (HP1–5), all lying in the coding sequence (Fig 7C–C' and Fig EV5A–D). To investigate whether these structures could be substrate for the Microprocessor function, we cloned each of the five HP, plus one sequence containing the first two HPs (which are very close to each other), downstream of *Renilla* luciferase (RL) in the psiCheck-2 plasmid (encoding also for firefly luciferase (FL) used for normalization, Fig EV5E) and transfected them in N2A cells. Knockdown of *Dgcr8* and *Drosha* (Fig 7D and E) did not alter RL/FL ratio in cells transfected with control (empty, Fig 7F) plasmid. In contrast, *Dgcr8* and *Drosha* knockdown increased RL/FL ratio in cells transfected with psiCheck-2 plasmids

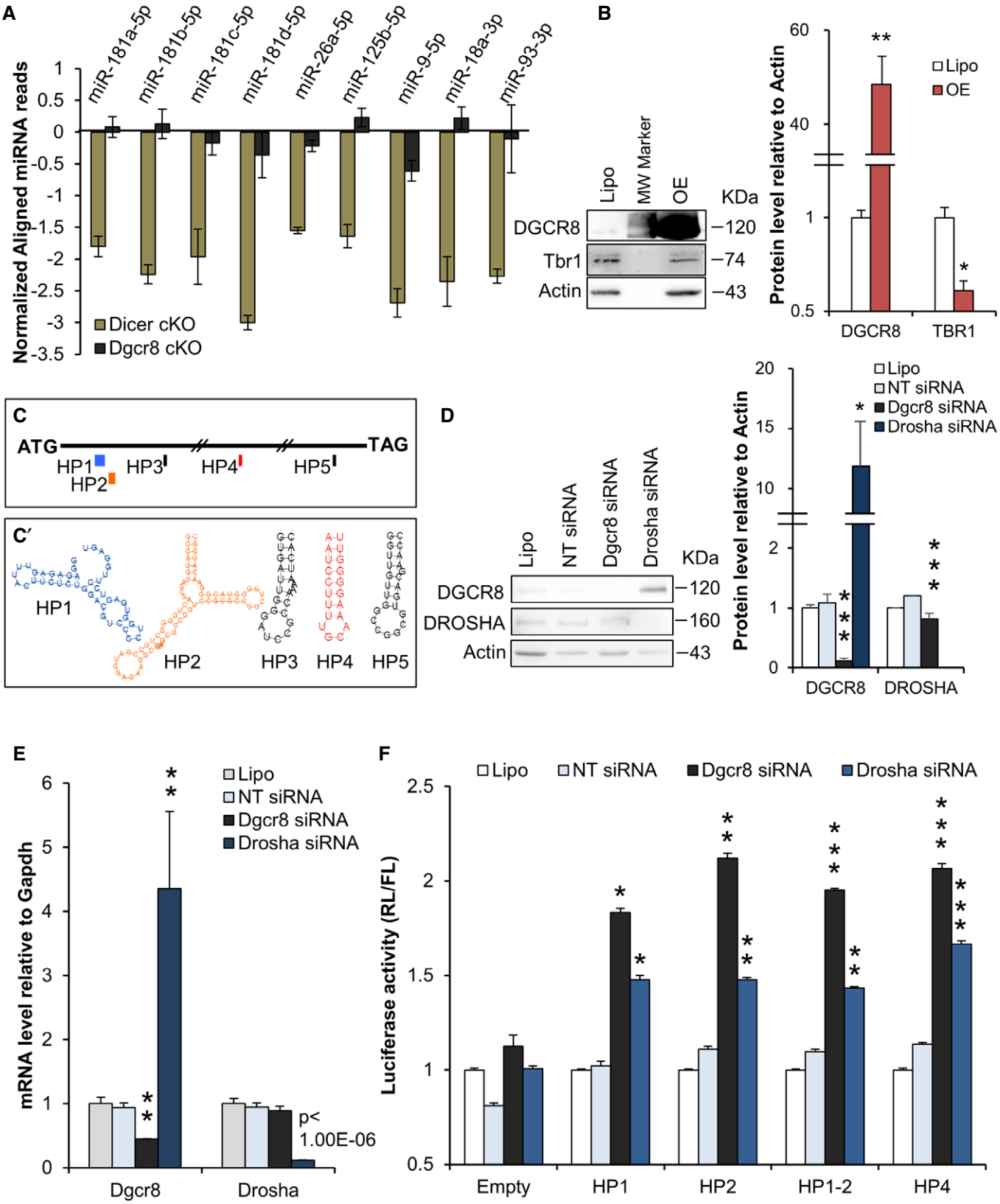

Figure 7.

Figure 7. The Microprocessor regulates Tbr1 expression likely by targeting evolutionarily conserved hairpin structures in its transcript.

A Read counts of experimentally validated miRNAs targeting the *Tbr1* transcript in E13.5 *Dicer* cKO and *Dgcr8* cKO cortices.

B Western blot and quantification of DGCR8, TBR1, and actin expression in N2A cells upon DGCR8 overexpression.

C Position of the 5 predicted hairpins (HPs) in *Tbr1* mRNA coding sequence (ATG-TAG, black thin segment).

C' Predicted secondary structures of the 5 HPs (color code as in C).

D Western blot and quantification of DGCR8, DROSHA, and actin expression in N2A cells upon *Dgcr8* or *Drosha* knockdown.

E qRT–PCR analysis of endogenous *Dgcr8* and *Drosha* mRNA in N2A cells upon *Dgcr8* or *Drosha* knockdown.

F N2A cells transfected with *Dgcr8*, *Drosha*, or control (NT) siRNAs, respectively, co-transfected with vectors described in (C) and (C').

Data information: Mock (Lipo); DGCR8 overexpression (OE); non-target (NT) siRNA. Bars indicate the variation from the mean (SEM; $n = 3$ biological replicas), and *P*-values are indicated (paired Student's *t*-test); *$P < 0.05$; **$P < 0.01$; ***$P < 0.001$.

containing HP1 (>16%), HP2 (>40%), HP1-2 (>45%), or HP4 (>53%), respectively (Fig 7F). These data suggest that the Microprocessor complex can exert a repressive function on *Tbr1* mRNA by a post-transcriptional/miRNA-independent mechanism.

Discussion

Our study clearly demonstrates that DGCR8 exerts essential functions in corticogenesis that are non-overlapping with those of DICER. Indeed, for the first time in the nervous system, here we show that conditional ablation of *Dgcr8* results in a more premature and severe phenotype compared to *Dicer*. In particular, we find that *Dgcr8* is essential for progenitor pools maintenance and differentiation during early corticogenesis. Remarkably, these distinct phenotypes are not paralleled by a greater depletion of miRNAs upon *Dgcr8* ablation compared to *Dicer*. Moreover, our data suggest that the Microprocessor complex can regulate TBR1 expression by a post-transcriptional/miRNA-independent mechanism. Thereby, here we propose that miRNA-independent functions of DGCR8 are critically required for proper corticogenesis.

Mutants for miRNA biogenesis genes, such as *Drosha*, *Dgcr8*, *Dicer,* and *Ago*(s) are a widely used approach to infer miRNA functions *in vivo,* reviewed in [9]. However, based on the assumption that mutants for genes that share common pathways result in similar phenotypes, and on the prevailing knowledge that canonical miRNAs account for the vast majority of the total miRNAs [23], most of these studies did not perform comparative studies on different knockouts in brain. Moreover, the few comparative studies in brain or other tissues/cell types have so far revealed milder or equal phenotypes in Microprocessor mutants compared to *Dicer* mutants [27]. Here, by showing that *Dgcr8* and *Dicer* mutants have distinct non-overlapping phenotypes in the developing telencephalon, we demonstrate that the impact of alternative/miRNA-independent functions of the Microprocessor [21,24,28,30,60–65,68] has been so far underestimated in corticogenesis. Our study thus paves the way to further comparative investigations of *Dgcr8* vs. *Dicer* mutants in other developmental times/tissues.

Our results indicate that *Dgcr8* deletion alters NPCs proliferation and leads to a dramatic overproduction of Tbr1 (and TUJ1)-positive neurons [36,38]. Specifically, the premature cell cycle exit of BPs accounts for the overproduction of these neurons upon conditional knockout of *Dgcr8*. Thus, here we postulate that in early corticogenesis DGCR8 might control the maintenance of APs/BPs pools to prevent their premature consumption, while DICER primarily controls the differentiation of newborn neurons [36]. This scenario would be consistent with the enriched expression pattern of *Dgcr8* mRNA in the VZ/SVZ and with the mild effect of *Dicer* depletion on NPCs expansion [36 and this study].

Our data suggest that DGCR8 regulates TBR1 level post-transcriptionally, possibly by targeting hairpin structures in its transcript, thus extending the emerging notion that alternative functions of the Microprocessor are required for corticogenesis [30]. However, and differently from the study of Knuckles *et al*, we did not find any difference in Ngn2 levels. This result might be explained by the existence of distinct Microprocessor complexes, bearing different affinities for targets (such as pri-miRNAs or mRNAs or subsets). Indeed, a recent study indicated that TDP-43 (TAR DNA-binding protein 43), a RNA-binding protein implicated in RNA metabolism and accessory component of Microprocessor complex, may be the factor that regulates the affinity of DROSHA complex for Ngn2 mRNA in cells undergoing neuronal differentiation. Interestingly, TDP-43 was dispensable for DROSHA-mediated DGCR8 regulation, whereas it was essential for Ngn2 expression control [68]. We therefore speculate that DGCR8 and TDP-43 might form distinct Microprocessor complexes, with different affinities for certain target RNAs that, by influencing the target-specificity of DROSHA cleavage, fine tune cortical neurogenesis. Further studies will be needed to identify targets and mechanisms of these DGCR8-dependent regulations in cortical development. Moreover, here we also provide novel insight of different miRNAs biogenesis pathways during cortical development. In particular, we find that, in contrast to other tissues/cell types where canonical miRNAs typically account for about 90% of the total [23], the proportions of canonical and non-canonical miRNAs seem roughly similar in developing cortex. This potentially remarkable finding, however, warrants future validation, given that the incomplete depletion of DGCR8 protein (e.g., below detection limit of the anti-DGCR8 immuno-blotting, see Fig 1) might account in part for the residual miRNAs observed in *Dgcr8* cKO mice.

Finally, our results have crucial implications for the study of the DiGeorge syndrome (also known as 22q11.2 deletion syndrome). This syndrome is caused by the hemizygous deletion of several genes, among which *Dgcr8* [69]; it is characterized by altered corticogenesis, neurogenesis [70], and cognitive deficits, among other symptoms [71]. However, so far the haploinsufficiency of *Dgcr8* or miRNAs has not been addressed as cause of early cortical defects. Perhaps, the investigation of alternative miRNA-independent function of DGCR8 in mouse models of DiGeorge syndrome might shed new light toward the identification of the molecular mechanism underlying defective corticogenesis of one of the most common genetic syndromes in humans.

Materials and Methods

Mouse lines and genotyping

Mice were housed under standard conditions at Istituto Italiano di Tecnologia (IIT), Genoa, Italy. All experiments and procedures were approved by the Italian Ministry of Health (Permits No. 057/2013 and 214/2015-PR) and IIT Animal Use Committee, in accordance with the Guide for the Care and Use of Laboratory Animals of the European Community Council Directives. *Emx1*$^{Cre/wt}$ knock-in mice [34] were crossed with *Dicer*$^{flox/flox}$ mice [33] and genotyped, as previously described [36]. *Dgcr8*$^{flox/flox}$ mice [32] were crossed with *Emx1*$^{Cre/wt}$ knock-in mice to obtain *Dgcr8*$^{flox/wt}$/*Emx1*$^{Cre/wt}$. Conditional ablation of *Dgcr8* gene was performed by crossing *Dgcr8*$^{flox/flox}$ mice with *Dgcr8*$^{flox/wt}$ *Emx1*$^{Cre/wt}$ mice. Mice resulting from these crossings were used for the experiments and are listed hereunder: *Dgcr8*$^{flox/wt}$ *Emx1*$^{wt/wt}$, *Dgcr8*$^{flox/flox}$ *Emx1*$^{wt/wt}$ (controls); *Dgcr8*$^{flox/wt}$ *Emx1*$^{Cre/wt}$ (conditional *Dgcr8* heterozygous); *Dgcr8*$^{flox/flox}$ *Emx1*$^{Cre/wt}$ (conditional *Dgcr8* knockout). *Dgcr8*-flox and WT alleles were genotyped by PCR with the following primers: *Dgcr8*-Fwd 5′-GACATCAATCTGAGTAGAGACAGG-3′ and *Dgcr8*-Rev 5′-CAGATGGTAACTAACCTGCCAACC-3′, annealed at 60°C and resulting in PCR fragments of 244 (WT) or 370 (flox) base pairs. For timed mating vaginal plug day was defined as E0.5.

BrdU labeling, immunofluorescence, *in situ* hybridization, and imaging

BrdU labeling was carried out by intraperitoneal injections of pregnant females at the indicated dpc as previously published [36]. Mice were sacrificed at the indicated time points after the first BrdU injection. Coronal cryosections (18–20 μm) through the fixed brains were prepared at the indicated ages, and processed for immunofluorescence or *in situ* hybridization on brain cryosections was performed as previously described [36]. Immunofluorescence was performed by re-hydrating cryosections in 1× PBS and subsequently permeabilizing them with progressive steps in 0.3–0.1% Triton in 1× PBS (PBST). Cryosections were subjected to antigen retrieval (when specified, Table EV2) with 10 mM citric acid at pH 6.0 for 10 min at 95°C, followed by 20–30 minutes of cooling and extensive washing in 0.1% PBST at RT. Blocking was performed in 0.1% PBST/5% normal goat serum for 1 h. Sections were then incubated with primary antibodies diluted in blocking solution for 14–16 h at 4°C in the darkness, washed extensively, and incubated with secondary antibodies diluted in blocking solution for 2 h. Progressive washing steps in 0.1% PBST and then 1× PBS were performed, and sections were incubated with Hoechst (1:300 in 1× PBS from a stock solution of 1 mg/ml in dimethyl sulfoxide, DMSO, Sigma) for 30 min in the darkness, extensively washed in 1× PBS, mounted with ProLong Gold Antifade (Invitrogen), air-dried overnight in the darkness, and sealed with nail polish (Electron Microscopy Sciences). For BrdU staining, the procedure above described was applied with modifications: after the first steps of hydration, the sections were (when specified) directly subjected to antigen retrieval with 100 μM citric acid for 30 min at 80°C, followed by cooling down for 20–30 min. BrdU unmasking was performed by incubating cryosections in 2N HCl for 30 minutes at 30.2°C, followed by extensive washing in 1× PBS. Antibodies and conditions are specified in Table EV2. Brain slices were mounted with ProLong Gold Antifade (Invitrogen-Thermo Fisher Scientific) and coverslipped. Fluorescence images were acquired with BX51 microscope (Olympus) equipped with Neurolucida stage and software (MBF Bioscience), or with LiveScan Swept Field Confocal Microscope (SFC), Nikon and analyzed with Nikon software version 4.11.0 (NIS Elements Viewer), ImageJ version 1.48u (Wayne Rasband, National Institutes of Health, USA), or Photoshop CS4 (Adobe). Black boxes were added outside the cortical tissue subjected to the analysis in immunofluorescence images in order to cover debris or tissue from the contralateral hemisphere or, in the case of *Dgcr8* cKO embryonic neocortices (smaller than control littermates), to prepare figure panels with identical size. *In situ* hybridization on brain cryosections was performed as previously described [36] with minor changes. Riboprobes for *Dgcr8* and *Dicer* were synthesized from PCR-amplified cDNAs with SP6 and T7 RNA polymerases (Promega) with DIG-labeled nucleotides (Roche) following manufacturer's instructions. Probes were purified with RNAeasy mini kit (Qiagen) following manufacturer's instructions. Probes were used at the final concentration of 50 ng/ml in hybridization solution, pre-hybridization, hybridization, and washing steps were performed at 70°C.

Quantification and analysis of embryonic dorsal telencephalon immunofluorescence images

Immunopositive cells for the indicated markers were counted through the depth of the telencephalic wall, and their numbers expressed as a proportion of total cell populations as indicated in figures and legends. For all the presented quantifications, data from each condition are the mean of 18 counted fields per condition (three embryos, three cryosections along the rostro-caudal axis per embryo, two fields per cryosections). The cortical wall thickness was estimated to the nearest 12.5 μm along the side of each counting; three brains were counted per condition; three sections along the rostro-caudal axis were counted per brain. For the evaluation of the ventricular length, the distance from the pallial–subpallial boundary to the dorsal-most point of the telencephalon was measured; three brains were counted per condition; three sections along the rostro-caudal axis were counted per brain. For cells counts, comparisons between control and *Dgcr8*-ablated or *Dicer*-ablated animals involved littermate or aged matched embryos; considering the size differences between control and *Dgcr8*- or *Dicer*-ablated embryonic dorsal telencephalon that emerged during development, care was taken that corresponding regions were analyzed and that the fields compared covered the same amount of ventricular surface.

Fluorescence-activated cell sorting (FACS), RNA extraction, cDNA preparation, and quantitative real-time PCR

To assess *Dgcr8*^{flox} recombination, *Dicer*^{flox} *Emx1*^{Cre} and *Dgcr8*^{flox} *Emx1*^{Cre} mice were crossed with Td-*Tomato*$^{flox/flox}$ mice (Jackson laboratory stock number 007908) [72]. Cortices were dissociated with the Neural Tissue Dissociation Kit (P) 130-092-628 (Miltenyi). Cells were collected from E13.5 embryos and were sorted by FACS, separating Tomato^{+} from Tomato^{-} subpopulations.

For miRNA profiling, total RNA was extracted from the dorsal telencephalon of WT, *Dgcr8* cHET, *Dgcr8* cKO, and *Dicer* cKO E13.5

littermate embryos (two embryos per condition) with RNeasy micro kit (Qiagen) according to the manufacturer's instructions. Total RNA was extracted from FACS-sorted Tomato$^+$ cells of E13.5 WT, and *Dicer* cKO and *Dgcr8* cKO embryos and N2A cells using QIAzol lysis reagent (Qiagen). Synthesis of cDNA from total RNA was performed with ImProm-II™ Reverse Transcription System (Promega). Quantitative real-time PCR (qRT–PCR) was performed using Quantifast SYBR Green method (Qiagen) with probes listed in Table EV3. Expression analysis was performed using the comparative cycle threshold (Ct) method.

Deep sequencing and analysis of small RNAs

The Illumina® TruSeq™ Small RNA Sample preparation kit was used to prepare and sequence total small RNA species, following manufacturer's instructions. Sequencing pipeline was performed at the Center for Genomic Science of IIT@SEMM as previously published [73]. Among small RNAs classes, snoRNAs proportions were stable between the samples and thus were chosen for normalization. We determined the enzyme dependencies for the genome-aligned miRNA sequences reads to which at least 50 reads from the WT data set mapper: Those were identified as miRNAs robustly expressed and evaluated according to the read number from WT versus mutant samples. Canonical and non-canonical miRNAs were then evaluated according to the read number obtained in WT samples and then classified according to their processing dependencies in mutant samples. The DGCR8 and Dicer dependences of miRNAs were then considered concurrently. To classify each miRNA as Dicer- and DGCR8-dependent (i.e., canonical), we required at least a -1.5 $\log_2$ fold regulation decrease in the number of reads in *Dicer* cKO mutant background, and at least -0.25 $\log_2$ fold regulation decrease in the number of reads in *Dgcr8* cKO mutant background. To classify each miRNA as Dicer-dependent and DGCR8-independent (i.e., non-canonical), we required at least a -1.5 $\log_2$ fold regulation decrease in the number of reads in *Dicer* cKO mutant background, and more than -0.25 $\log_2$ fold regulation decrease in the number of reads in *Dgcr8* cKO mutant background. The analysis of Tbr1-targeting miRNAs (predicted or experimentally associated) was conducted with the three software packages TarBase, TargetScan (taking in account only miRNAs having at least a context score of -0.2), and miRanda [74,75]. The deep-sequencing data from this publication have been submitted to the NCBI GEO database [76] assigned the identifier GSE82069.

Plasmids and cloning

The putative *Tbr1* hairpin sequences were identified as previously described [30] taking advantage of EvoFold [77], with the secondary structure prediction program RNAfold [78] and cloned between the *Renilla* luciferase coding region and its synthetic poly(A) in the psiCheck-2 plasmid (Promega) by GeneArt™ (Thermo Fisher Scientific). *Dgcr8* cDNA was PCR amplified and cloned into pCAGGS vector.

Cell culture, transfection, luciferase assay, and Western blotting

N2A cells were maintained at standard conditions, 50 nM of control siRNAs, or *Dgcr8* or *Drosha* siRNA (cat # D-001206-14, M-051364-00, M-065630-03 Dharmacon) were reverse transfected with Lipofectamine 2000 (Invitrogen), according to the manufacturer's protocol. The next day, cells were transfected with psiCheck-2 vectors. Two days after siRNA transfection, cells were harvested for RNA extraction or lysed for analysis of *Renilla* and firefly luciferase activities with Dual Luciferase Assay System (Promega). For total protein extraction, embryonic neocortices or cell pellets were homogenized in RIPA buffer. Cortices were sonicated (10 short pulses) and left on ice for 15 min. Neocortices or cell pellets were clarified by centrifugation at 20,000 *g*, and the protein concentration was determined using a Bradford Assay kit (Bio-Rad). For blot analysis, equal amounts of protein were run on Mini-PROTEAN® TGX™ Precast Gels (Bio-Rad) and transferred on nitrocellulose membranes (GE Healthcare). Membranes were probed with rabbit anti-DGCR8 (Proteintech, 10996-1-AP, 1:1,000), rabbit anti-DROSHA (Cell Signaling, D28B1; 1:1,000), rabbit anti Tbr1 (Abcam, ab31940; 1:1,000), and rabbit anti-actin (Sigma, A2066; 1:5,000) followed by HRP-conjugated secondary antibody anti-rabbit (Invitrogen, A16104; 1:2,000). LAS 4000 Mini Imaging System (GE Healthcare) was used to digitally acquire chemiluminescence signals, and the band intensities were quantified using Fiji. The specificity of antibodies to DGCR8 and DROSHA was verified on N2A cells transfected with *Dgcr8* siRNA or *Drosha* siRNA, respectively.

Statistical analysis

Data are expressed as mean ± standard error of the mean (SEM) for all quantifications and assays. Differences between groups were tested for statistical significance, where appropriate using one-way analysis of variance (ANOVA) or two-way ANOVA followed by Tukey's *post hoc* testing. Statistical analysis of luciferase assays results was conducted by two-tailed paired Student's *t*-test. Significance was expressed as follows: **P*-value < 0.05; ***P*-value < 0.01; ****P*-value < 0.001; *****P*-value < 0.0001; n.s., not significant.

Expanded View for this article is available online.

Acknowledgements

We thank Drs. G Hannon (Cold Spring Harbor Laboratory, MA, USA), E. Fuchs (Rockefeller Univ. NY, USA), and S. Itohara (RIKEN, Wako, Japan) for kindly providing *Dicer*-flox, *Dgcr8*-flox, and *Emx1*-Cre mouse lines, respectively. We thank Dr. M. Nanni, C. Gasperini, and the IIT-NBT technical staff (Drs. M. Pesce and E. Albanesi) for help with some experiments, and the staff of IIT Animal Facility (F. Piccardi, and Dr. M. Morini) for excellent assistance in animal experiments. We thank Dr. E. Taverna (Max Planck Institute for Evolutionary Anthropology, Germany) for critical reading of the manuscript. FN was supported by the European Research Executive Agency (REA) through the FP7-PEOPLE-2010-RG "miRNAs/22q11DS" (No. 268298). DDPT and FN were supported by intramural funds of Fondazione Istituto Italiano di Tecnologia (IIT).

Author contributions

DDPT conceived, supervised, and coordinated the project. FNio Co-supervised FM during the initial experiments. Investigation: FM performed all the experiments; NH carried out the experiments in Figs 4, 5A–H and EV3M–N; RP performed the Western blots in Figs 1 and 7; MJM carried out and analyzed deep-sequencing experiments under FN supervision; FM prepared all the

Figures; HA prepared the data in Figs 6C and EV4A; FM and HA performed the Formal Analysis; DDPT and FM co-wrote the manuscript. All authors approved the final version of the manuscript.

Conflict of interest

The authors declare that they have no conflict of interest.

References

1. Kriegstein A, Noctor S, Martínez-Cerdeño V (2006) Patterns of neural stem and progenitor cell division may underlie evolutionary cortical expansion. *Nat Rev Neurosci* 7: 883 – 890
2. Taverna E, Götz M, Huttner WB (2014) The cell biology of neurogenesis: toward an understanding of the development and evolution of the neocortex. *Annu Rev Cell Dev Biol* 30: 465 – 502
3. Lee RC, Feinbaum RL, Ambros V (1993) The *C. elegans* heterochronic gene lin-4 encodes small RNAs with antisense complementarity to lin-14. *Cell* 75: 843 – 854.
4. Reinhart BJ, Slack FJ, Basson M, Pasquinelli AE, Bettinger JC, Rougvie AE, Horvitz HR, Ruvkun G (2000) The 21-nucleotide let-7 RNA regulates developmental timing in *Caenorhabditis elegans*. *Nature* 403: 901 – 906
5. Pasquinelli AE, Reinhart BJ, Slack F, Martindale MQ, Kuroda MI, Maller B, Hayward DC, Ball EE, Degnan B, Müller P *et al* (2000) Conservation of the sequence and temporal expression of let-7 heterochronic regulatory RNA. *Nature* 408: 86 – 89
6. Wightman B, Ha I, Ruvkun G (1993) Posttranscriptional regulation of the heterochronic gene lin-14 by lin-4 mediates temporal pattern formation in *C. elegans*. *Cell* 75: 855 – 862
7. Friedman RC, Farh KK-H, Burge CB, Bartel DP (2009) Most mammalian mRNAs are conserved targets of microRNAs. *Genome Res* 19: 92 – 105
8. Aksoy-Aksel A, Zampa F, Schratt G (2014) MicroRNAs and synaptic plasticity–a mutual relationship. *Philos Trans R Soc Lond B Biol Sci* 369: 20130515
9. Barca-Mayo O, De Pietri Tonelli D (2014) Convergent microRNA actions coordinate neocortical development. *Cell Mol Life Sci* 71: 2975 – 2995
10. Filipowicz W, Sonenberg N (2015) The long unfinished march towards understanding microRNA-mediated repression. *RNA* 21: 519 – 524
11. Ha M, Kim VN (2014) Regulation of microRNA biogenesis. *Nat Rev Mol Cell Biol* 15: 509 – 524
12. Krol J, Loedige I, Filipowicz W (2010) The widespread regulation of microRNA biogenesis, function and decay. *Nat Rev Genet* 11: 597 – 610
13. Denli AM, Tops BBJ, Plasterk RHA, Ketting RF, Hannon GJ (2004) Processing of primary microRNAs by the Microprocessor complex. *Nature* 432: 231 – 235
14. Gregory RI, Yan K-P, Amuthan G, Chendrimada T, Doratotaj B, Cooch N, Shiekhattar R (2004) The Microprocessor complex mediates the genesis of microRNAs. *Nature* 432: 235 – 240
15. Han J, Lee Y, Yeom K-H, Kim Y-K, Jin H, Kim VN (2004) The Drosha-DGCR8 complex in primary microRNA processing. *Genes Dev* 18: 3016 – 3027
16. Landthaler M, Yalcin A, Tuschl T (2004) The human DiGeorge syndrome critical region gene 8 and Its *D. melanogaster* homolog are required for miRNA biogenesis. *Curr Biol* 14: 2162 – 2167
17. Shenoy A, Danial M, Blelloch RH (2015) Let-7 and miR-125 cooperate to prime progenitors for astrogliogenesis. *EMBO J* 34: 1180 – 1194
18. Zhang C, Ge X, Liu Q, Jiang M, Li MW, Li H (2015) MicroRNA-mediated non-cell-autonomous regulation of cortical radial glial transformation revealed by a Dicer1 knockout mouse model. *Glia* 63: 860 – 876
19. Petri R, Malmevik J, Fasching L, Åkerblom M, Jakobsson J (2014) MiRNAs in brain development. *Exp Cell Res* 321: 84 – 89
20. Howng S-YB, Huang Y, Ptáček L, Fu Y-H (2015) Understanding the role of dicer in astrocyte development. *PLoS One* 10: e0126667
21. Babiarz JE, Hsu R, Melton C, Thomas M, Ullian EM, Blelloch R (2011) A role for noncanonical microRNAs in the mammalian brain revealed by phenotypic differences in Dgcr8 versus Dicer1 knockouts and small RNA sequencing. *RNA* 17: 1489 – 1501
22. Babiarz JE, Ruby JG, Wang Y, Bartel DP, Blelloch R (2008) Mouse ES cells express endogenous shRNAs, siRNAs, and other Microprocessor-independent, Dicer-dependent small RNAs. *Genes Dev* 22: 2773 – 2785
23. Castellano L, Stebbing J (2013) Deep sequencing of small RNAs identifies canonical and non-canonical miRNA and endogenous siRNAs in mammalian somatic tissues. *Nucleic Acids Res* 41: 3339 – 3351
24. Dhir A, Dhir S, Proudfoot NJ, Jopling CL (2015) Microprocessor mediates transcriptional termination in genes encoding long noncoding microRNAs. *Nat Struct Mol Biol* 22: 319 – 327
25. Wang Y, Medvid R, Melton C, Jaenisch R, Blelloch R (2007) DGCR8 is essential for microRNA biogenesis and silencing of embryonic stem cell self-renewal. *Nat Genet* 39: 380 – 385
26. Macias S, Cordiner RA, Gautier P, Plass M, Cáceres JF (2015) DGCR8 acts as an adaptor for the exosome complex to degrade double-stranded structured RNAs. *Mol Cell* 60: 873 – 885
27. Yang J-S, Lai EC (2011) Alternative miRNA biogenesis pathways and the interpretation of core miRNA pathway mutants. *Mol Cell* 43: 892 – 903
28. Gromak N, Dienstbier M, Macias S, Plass M, Eyras E, Cáceres JF, Proudfoot NJ (2013) Drosha regulates gene expression independently of RNA cleavage function. *Cell Rep* 5: 1499 – 1510
29. Hsu R, Schofield CM, Dela Cruz CG, Jones-Davis DM, Blelloch R, Ullian EM (2012) Loss of microRNAs in pyramidal neurons leads to specific changes in inhibitory synaptic transmission in the prefrontal cortex. *Mol Cell Neurosci* 50: 283 – 292
30. Knuckles P, Vogt MA, Lugert S, Milo M, Chong MMW, Hautbergue GM, Wilson SA, Littman DR, Taylor V (2012) Drosha regulates neurogenesis by controlling neurogenin 2 expression independent of microRNAs. *Nat Neurosci* 15: 962 – 969
31. Götz M, Huttner WB (2005) The cell biology of neurogenesis. *Nat Rev Mol Cell Biol* 6: 777 – 788
32. Yi R, Pasolli HA, Landthaler M, Hafner M, Ojo T, Sheridan R, Sander C, O'Carroll D, Stoffel M, Tuschl T *et al* (2009) DGCR8-dependent microRNA biogenesis is essential for skin development. *Proc Natl Acad Sci USA* 106: 498 – 502
33. Murchison EP, Partridge JF, Tam OH, Cheloufi S, Hannon GJ (2005) Characterization of Dicer-deficient murine embryonic stem cells. *Proc Natl Acad Sci USA* 102: 12135 – 12140
34. Iwasato T, Datwani A, Wolf AM, Nishiyama H, Taguchi Y, Tonegawa S, Knöpfel T, Erzurumlu RS, Itohara S (2000) Cortex-restricted disruption of NMDAR1 impairs neuronal patterns in the barrel cortex. *Nature* 406: 726 – 731
35. Davis TH, Cuellar TL, Koch SM, Barker AJ, Harfe BD, McManus MT, Ullian EM (2008) Conditional loss of Dicer disrupts cellular and tissue morphogenesis in the cortex and hippocampus. *J Neurosci* 28: 4322 – 4330
36. De Pietri Tonelli D, Pulvers JN, Haffner C, Murchison EP, Hannon GJ, Huttner WB (2008) miRNAs are essential for survival and differentiation of newborn neurons but not for expansion of neural progenitors during early neurogenesis in the mouse embryonic neocortex. *Development* 135: 3911 – 3921

37. Hong J, Zhang H, Kawase-Koga Y, Sun T (2013) MicroRNA function is required for neurite outgrowth of mature neurons in the mouse postnatal cerebral cortex. *Front Cell Neurosci* 7: 151
38. Kawase-Koga Y, Otaegi G, Sun T (2009) Different timings of Dicer deletion affect neurogenesis and gliogenesis in the developing mouse central nervous system. *Dev Dyn* 238: 2800 – 2812
39. Li Q, Bian S, Hong J, Kawase-Koga Y, Zhu E, Zheng Y, Yang L, Sun T (2011) Timing specific requirement of microRNA function is essential for embryonic and postnatal hippocampal development. *PLoS One* 6: e26000
40. Makeyev EV, Zhang J, Carrasco MA, Maniatis T (2007) The MicroRNA miR-124 promotes neuronal differentiation by triggering brain-specific alternative pre-mRNA splicing. *Mol Cell* 27: 435 – 448
41. McLoughlin HS, Fineberg SK, Ghosh LL, Tecedor L, Davidson BL (2012) Dicer is required for proliferation, viability, migration and differentiation in corticoneurogenesis. *Neuroscience* 223: 285 – 295
42. Nowakowski TJ, Mysiak KS, Pratt T, Price DJ (2011) Functional dicer is necessary for appropriate specification of radial glia during early development of mouse telencephalon. *PLoS One* 6: e23013
43. Saurat N, Andersson T, Vasistha NA, Molnár Z, Livesey FJ (2013) Dicer is required for neural stem cell multipotency and lineage progression during cerebral cortex development. *Neural Dev* 8: 14
44. Galluzzi L, Aaronson SA, Abrams J, Alnemri ES, Andrews DW, Baehrecke EH, Bazan NG, Blagosklonny MV, Blomgren K, Borner C *et al* (2009) Guidelines for the use and interpretation of assays for monitoring cell death in higher eukaryotes. *Cell Death Differ* 16: 1093 – 1107
45. Menezes JR, Luskin MB (1994) Expression of neuron-specific tubulin defines a novel population in the proliferative layers of the developing telencephalon. *J Neurosci* 14: 5399 – 5416
46. Bani-Yaghoub M, Tremblay RG, Lei JX, Zhang D, Zurakowski B, Sandhu JK, Smith B, Ribecco-Lutkiewicz M, Kennedy J, Walker PR *et al* (2006) Role of Sox2 in the development of the mouse neocortex. *Dev Biol* 295: 52 – 66
47. Götz M, Barde Y-A (2005) Radial glial cells defined and major intermediates between embryonic stem cells and CNS neurons. *Neuron* 46: 369 – 372
48. Englund C, Fink A, Lau C, Pham D, Daza RAM, Bulfone A, Kowalczyk T, Hevner RF (2005) Pax6, Tbr2, and Tbr1 are expressed sequentially by radial glia, intermediate progenitor cells, and postmitotic neurons in developing neocortex. *J Neurosci* 25: 247 – 251
49. Hevner RF, Shi L, Justice N, Hsueh Y-P, Sheng M, Smiga S, Bulfone A, Goffinet AM, Campagnoni AT, Rubenstein JL (2001) Tbr1 regulates differentiation of the preplate and layer 6. *Neuron* 29: 353 – 366
50. Hanna-Morris A, Badvie S, Cohen P, McCullough T, Andreyev HJN, Allen-Mersh TG (2009) Minichromosome maintenance protein 2 (MCM2) is a stronger discriminator of increased proliferation in mucosa adjacent to colorectal cancer than Ki-67. *J Clin Pathol* 62: 325 – 330
51. Caviness VS, Takahashi T, Nowakowski RS (1995) Numbers, time and neocortical neuronogenesis: a general developmental and evolutionary model. *Trends Neurosci* 18: 379 – 383
52. Takahashi T, Nowakowski RS, Caviness VS (1995) The cell cycle of the pseudostratified ventricular epithelium of the embryonic murine cerebral wall. *J Neurosci* 15: 6046 – 6057
53. Ochiai W, Nakatani S, Takahara T, Kainuma M, Masaoka M, Minobe S, Namihira M, Nakashima K, Sakakibara A, Ogawa M *et al* (2009) Periventricular notch activation and asymmetric Ngn2 and Tbr2 expression in pair-generated neocortical daughter cells. *Mol Cell Neurosci* 40: 225 – 233
54. Mattar P, Langevin LM, Markham K, Klenin N, Shivji S, Zinyk D, Schuurmans C (2008) Basic helix-loop-helix transcription factors cooperate to specify a cortical projection neuron identity. *Mol Cell Biol* 28: 1456 – 1469
55. Lodato S, Arlotta P (2015) Generating neuronal diversity in the mammalian cerebral cortex. *Annu Rev Cell Dev Biol* 31: 699 – 720
56. Srinivasan K, Leone DP, Bateson RK, Dobreva G, Kohwi Y, Kohwi-Shigematsu T, Grosschedl R, McConnell SK (2012) A network of genetic repression and derepression specifies projection fates in the developing neocortex. *Proc Natl Acad Sci USA* 109: 19071 – 19078
57. Arlotta P, Molyneaux BJ, Chen J, Inoue J, Kominami R, Macklis JD (2005) Neuronal subtype-specific genes that control corticospinal motor neuron development *in vivo*. *Neuron* 45: 207 – 221
58. Chong MMW, Zhang G, Cheloufi S, Neubert TA, Hannon GJ, Littman DR (2010) Canonical and alternate functions of the microRNA biogenesis machinery. *Genes Dev* 24: 1951 – 1960
59. Moltzahn F, Olshen AB, Baehner L, Peek A, Fong L, Stöppler H, Simko J, Hilton JF, Carroll P, Blelloch R (2011) Microfluidic-based multiplex qRT-PCR identifies diagnostic and prognostic microRNA signatures in the sera of prostate cancer patients. *Cancer Res* 71: 550 – 560
60. Han J, Pedersen JS, Kwon SC, Belair CD, Kim Y-K, Yeom K-H, Yang W-Y, Haussler D, Blelloch R, Kim VN (2009) Posttranscriptional crossregulation between Drosha and DGCR8. *Cell* 136: 75 – 84
61. Luhur A, Chawla G, Wu Y-C, Li J, Sokol NS (2014) Drosha-independent DGCR8/Pasha pathway regulates neuronal morphogenesis. *Proc Natl Acad Sci USA* 111: 1421 – 1426
62. Macias S, Plass M, Stajuda A, Michlewski G, Eyras E, Cáceres JF (2012) DGCR8 HITS-CLIP reveals novel functions for the Microprocessor. *Nat Struct Mol Biol* 19: 760 – 766
63. Seong Y, Lim D-H, Kim A, Seo JH, Lee YS, Song H, Kwon Y-S (2014) Global identification of target recognition and cleavage by the Microprocessor in human ES cells. *Nucleic Acids Res* 42: 12806 – 12821
64. Triboulet R, Chang H-M, Lapierre RJ, Gregory RI (2009) Post-transcriptional control of DGCR8 expression by the Microprocessor. *RNA* 15: 1005 – 1011
65. Shenoy A, Blelloch R (2009) Genomic analysis suggests that mRNA destabilization by the Microprocessor is specialized for the auto-regulation of Dgcr8. *PLoS One* 4: e6971
66. Ganesan G, Rao SMR (2008) A novel noncoding RNA processed by Drosha is restricted to nucleus in mouse. *RNA* 14: 1399 – 1410
67. Karginov FV, Cheloufi S, Chong MMW, Stark A, Smith AD, Hannon GJ (2010) Diverse endonucleolytic cleavage sites in the mammalian transcriptome depend upon microRNAs, Drosha, and additional nucleases. *Mol Cell* 38: 781 – 788
68. Di Carlo V, Grossi E, Laneve P, Morlando M, Dini Modigliani S, Ballarino M, Bozzoni I, Caffarelli E (2013) TDP-43 regulates the Microprocessor complex activity during *in vitro* neuronal differentiation. *Mol Neurobiol* 48: 952 – 963
69. Drew LJ, Crabtree GW, Markx S, Stark KL, Chaverneff F, Xu B, Mukai J, Fenelon K, Hsu P-K, Gogos JA *et al* (2011) The 22q11.2 microdeletion: fifteen years of insights into the genetic and neural complexity of psychiatric disorders. *Int J Dev Neurosci* 29: 259 – 281
70. Meechan DW, Tucker ES, Maynard TM, LaMantia AS (2009) Diminished dosage of 22q11 genes disrupts neurogenesis and cortical development in a mouse model of 22q11 deletion/DiGeorge syndrome. *Proc Natl Acad Sci USA* 106: 16434 – 16445
71. Forstner AJ, Degenhardt F, Schratt G, Nöthen MM (2013) MicroRNAs as the cause of schizophrenia in 22q11.2 deletion carriers, and possible implications for idiopathic disease: a mini-review. *Front Mol Neurosci* 6: 47
72. Madisen L, Zwingman TA, Sunkin SM, Oh SW, Zariwala HA, Gu H, Ng LL, Palmiter RD, Hawrylycz MJ, Jones AR *et al* (2010) A robust and high-throughput Cre reporting and characterization system for the whole mouse brain. *Nat Neurosci* 13: 133 – 140

73. Muller H, Marzi MJ, Nicassio F (2014) IsomiRage: from Functional Classification to Differential Expression of miRNA Isoforms. *Front Bioeng Biotechnol* 2: 38
74. Lewis BP, Burge CB, Bartel DP (2005) Conserved seed pairing, often flanked by adenosines, indicates that thousands of human genes are microRNA targets. *Cell* 120: 15 – 20
75. Vergoulis T, Vlachos IS, Alexiou P, Georgakilas G, Maragkakis M, Reczko M, Gerangelos S, Koziris N, Dalamagas T, Hatzigeorgiou AG (2012) TarBase 6.0: capturing the exponential growth of miRNA targets with experimental support. *Nucleic Acids Res* 40: D222 – D229
76. Edgar R, Domrachev M, Lash AE (2002) Gene Expression Omnibus: NCBI gene expression and hybridization array data repository. *Nucleic Acids Res* 30: 207 – 210
77. Pedersen JS, Bejerano G, Siepel A, Rosenbloom K, Lindblad-Toh K, Lander ES, Kent J, Miller W, Haussler D (2006) Identification and classification of conserved RNA secondary structures in the human genome. *PLoS Comput Biol* 2: e33
78. Hofacker IL, Fontana W, Stadler PF, Bonhoeffer LS, Tacker M, Schuster P (1994) Fast folding and comparison of RNA secondary structures. *Monatshefte fur Chemie Chem Mon* 125: 167 – 188

